Accepted Manuscript

In vitro screening of 2-(1*H*-imidazol-1-yl)-1-phenylethanol derivatives as antiprotozoal agents and docking studies on *T. cruzi* CYP51

Daniela De Vita, Dr., Francesca Moraca, Claudio Zamperini, Fabiana Pandolfi, Roberto Di Santo, An Matheeussen, Louis Maes, Silvano Tortorella, Luigi Scipione

PII: S0223-5234(16)30108-8

DOI: 10.1016/j.ejmech.2016.02.028

Reference: EJMECH 8379

To appear in: *European Journal of Medicinal Chemistry*

Received Date: 7 October 2015

Revised Date: 18 January 2016

Accepted Date: 10 February 2016

Please cite this article as: D. De Vita, F. Moraca, C. Zamperini, F. Pandolfi, R. Di Santo, A. Matheeussen, L. Maes, S. Tortorella, L. Scipione, *In vitro* screening of 2-(1*H*-imidazol-1-yl)-1-phenylethanol derivatives as antiprotozoal agents and docking studies on *T. cruzi* CYP51, *European Journal of Medicinal Chemistry* (2016), doi: 10.1016/j.ejmech.2016.02.028.

In vitro screening of 2-(1*H*-imidazol-1-yl)-1-phenylethanol derivatives as antiprotozoal agents and docking studies on *T. cruzi* CYP51

Daniela De Vita,[a*] Francesca Moraca,[c] Claudio Zamperini,[c] Fabiana Pandolfi,[a] Roberto Di Santo,[a,b] An Matheeussen,[d] Louis Maes,[d] Silvano Tortorella[a] and Luigi Scipione[a]

[a] Department of "Chimica e Tecnologie del Farmaco", Sapienza University of Rome, Piazzale Aldo Moro, 5, 00185 Rome, Italy

[b] "Istituto Pasteur-Fondazione Cenci Bolognetti", Department of "Chimica e Tecnologie del Farmaco", Sapienza University of Rome, Piazzale Aldo Moro, 5, 00185 Rome, Italy

[c] Department of "Biotecnologie, Chimica e Farmacia", "University of Siena", Via A. Moro 2, 53100 Siena, Italy

[d] Laboratory for Microbiology, Parasitology and Hygiene (LMPH), Faculty of Pharmaceutical, Biomedical and Veterinary Sciences, Antwerp University, 2610 Antwerp, Belgium

* Corresponding author: Dr. Daniela De Vita, Department of "Chimica e Tecnologie del Farmaco", Sapienza University of Rome, Piazzale Aldo Moro, 5, 00185 Rome, Italy.

Email: daniela.devita@uniroma1.it

Graphical abstract

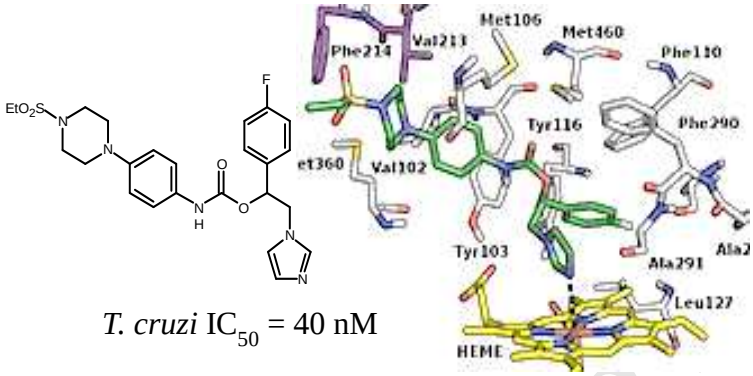

T. cruzi IC_{50} = 40 nM

Abstract

Sterol 14α-demethylase (CYP51) is a key enzyme involved in the survival and virulence of many parasite protozoa, such as *Trypanosoma* and *Leishmania* species, thus representing a valuable drug target for the treatment of Kinetoplastid diseases. A set of azole-based compounds selected from an in-house compound library was *in vitro* screened against different human protozoan parasites. Several compounds showed selective activity against *T. cruzi*, with compound **7** being the most active (IC_{50} = 40nM). Given the structural similarity between the compounds here reported and known CYP51 inhibitors, a molecular docking study was performed to assess their binding with protozoal target and to rationalize the biological activity data.

Highlights

- A number of azoles with selective activity against *T. cruzi* were identified.
- The most active compound possesses 40 nM IC_{50}.
- The biological activity of pure enantiomers was evaluated.
- Molecular docking on *T. cruzi* CYP51 was assessed to rationalize biological data.

Keywords

Trypanosoma cruzi; Azoles; CYP51.

1. Introduction

Trypanosoma cruzi (*T. cruzi*) is an intracellular protozoan parasite responsible for Chagas disease (CD), considered one of the neglected diseases [1]. It is transmitted to the mammalian host primarily by infected faeces of blood-sucking triatomine bugs, also known as “kissing bugs”. Other modes of transmission include infected blood transfusion, vertical transmission or infected organ transplantation [2]. CD occurs mainly in Latin America, however, the number of infections in the United States of America, Canada, many European and some Western Pacific countries continues to increase because of population mobility [3]. To date, CD treatment includes the nitro-derivatives benznidazole and nifurtimox [4]. Despite their significant activity in congenital and adult acute *T. cruzi* infections, their use presents major drawbacks, including long duration of therapy, poor efficacy in the chronic phase, different efficacy related to geographical area and several adverse reactions [5]. These facts motivate to continue the research and development of new more safe and effective drugs [6,7].

Sterol 14α-demethylase (CYP51) represents a main target to develop new drugs for the treatment of CD. This enzyme catalyzes the removal of 14α-methyl group of sterols, an essential step in sterol biosynthesis leading to the formation of cholesterol in vertebrates, ergosterol in fungi, and a variety of 24-alkylated ergosterol derivatives in plants and protozoa [8]. Unlike mammals that can accumulate cholesterol from diet, blocking of ergosterol production in fungi and protozoa is lethal: it affects cytokinesis, stops cell growth, and eventually leads to collapse of the cellular membrane [9]. Due to the similarity in sterol composition, several antifungal agents have been tested against *T. cruzi*. Among these, posaconazole and the ravuconazole prodrug E1224 have recently terminated Phase-2 clinical trials for treatment of chronic Chagas disease [10]. These studies have led to disappointing conclusions about their effectiveness in chronic CD, mailnly due to poor pharmacokinetic properties. Moreover, the chemical synthesis of posaconazole and ravuconazole is coumbersome and very expensive. Nevertheless, research for inhibitors specifically designed for the

CYP51 of *T. cruzi* ($CYP51_{Tc}$), less expensive and endowed with optimal pharmacokinetic properties, is still promising [11].

In previous studies [12, 13], we identified promising imidazole derivatives with a high and selective *in vitro* activity against intracellular amastigotes of *T. cruzi* (Tulahuen C2C4). The most potent among them (**I** - **III**) showed IC_{50}-values in the low nM range and are reported in Chart 1. These compounds were found to inhibit the *T. cruzi* sterol 14α-demethylase and, as demonstrated by the co-crystals, they fit into the deepest segment of the CYP51 cavity and disrupt the heme support from the protein moiety (compound **II**) or block the entrance into the CYP51 substrate access channel (compound **III**).

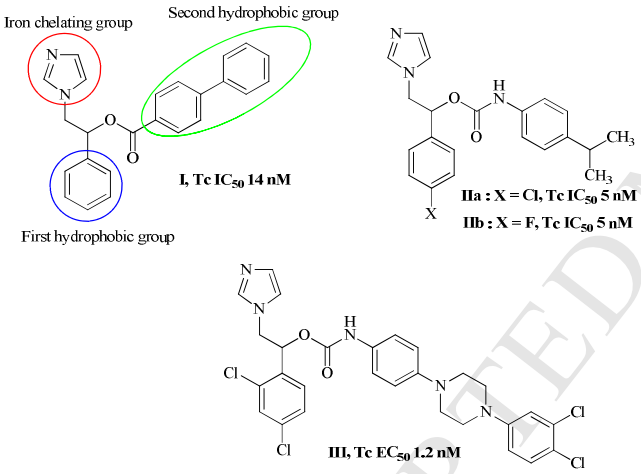

Chart 1: lead compounds identified in our previous studies

Here, we report the *in vitro* antiprotozoal activity evaluation of eight compounds selected from our in-house imidazole library; they are structurally correlated with already described **I** - **III** and some of them possess antifungal activity [14,15].

All selected molecules possess the three principal pharmacophoric features of CYP51 inhibitors: i) an iron chelating nitrogen containing heterocycle; ii) an hydrophobic group quite close to it; iii) a second hydrophobic group (Chart 1). Furthermore, we tried to rationalize the biological data by

means of a molecular docking study based on known crystal structures of *T. cruzi* CYP51 ($CYP51_{Tc}$).

Compounds **1** and **2** (logP 5.963 and 5.662 respectively) were chosen to verify how the presence of a halogen atom (chlorine or fluorine) on the first hydrophobic group influences the antiparasitic activity in comparison to compound **I** (logP 5.566). Compound **3** (logP 7.236) was chosen in order to verify the effect of more bulky and hydrophobic group in the same position. In addition, we have chosen compounds **4-8** to evaluate how side chains with different size and polarity in the second hydrophobic group affect the activity. In particular, compounds **5** (logP 4.405) and **6** (logP 4.138) possess a more polar piperazine moiety instead of the aromatic ring closer to carbonyl linker (**5** and **6** *vs* **I**); compound **4** (logP 3.775) with respect to **5** and **6** contains a more polar furoylpiperazine moiety, present in some compounds with antitrypanosomal activity [16,17]. Finally, compounds **7** (logP 4.096) and **8** (logP 5.011) have been selected for their similitude with compound **III** (logP 8.155) but with more polar groups in the terminal portion of the side chain

2. Results and discussion

2.1 Chemistry

Compounds **1**, **2, 4-8** were previously synthesized and evaluated for their antifungal activities [14,15]. The new compound **3** was prepared as previously reported for compounds **1** and **2** [15]. In brief, 1-(biphenyl-4-yl)-2-(1*H*-imidazol-1-yl)ethanol was activated as alcoholate using NaH in dry CH_3CN and then the biphenyl-4-carbonyl chloride was added (Scheme 1).

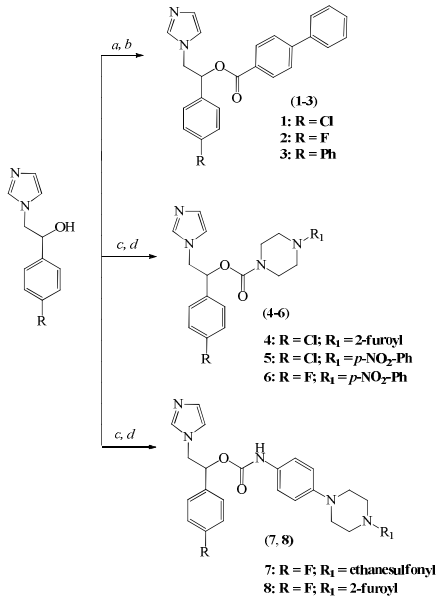

Scheme 1: Reagents and conditions for **1-8.** ***a***: NaH, CH_3CN, r.t., 2 h. ***b***: biphenyl-4-carbonyl chloride**.** ***c:*** dry CH_3CN, triphosgene, r.t., overnight; ***d:*** TEA, opportune amine, r.t., overnight.

The synthesis of **4-8** was accomplished by the activation of the –OH group of 2-(1*H*-imidazol-1-yl)-1-phenylethanol with triphosgene in dry CH_3CN to obtain the desired chloroformate; then TEA and the selected amines were added to the chloroformate stirring overnight (scheme 1) [14].

Commercially available amines were used to synthesize compounds **4-6**; otherwise the side chains of **7** and **8** were prepared as described in the Scheme 2**.** The synthesis of the amines **11 and 12** started by condensation of 1-fluoro-4-nitrobenzene with the appropriate commercial piperazine refluxed for 2h in CH_3CN. The obtained nitro compounds (**9** and **10**) were reduced to the corresponding amines (**11** and **12**) with 50 psi of H_2 for 4h in a Parr apparatus, using Pd/C (5%) as catalyst. All the selected compounds contain a chiral carbon atom and were obtained as racemic mixtures.

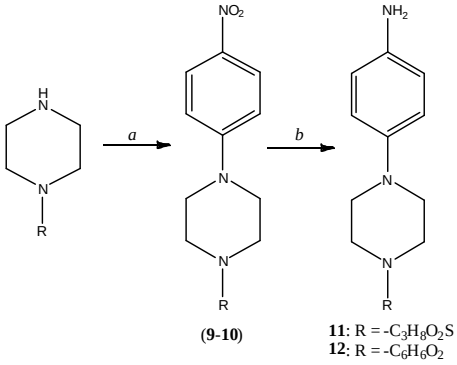

Scheme 2: Reagents and conditions. ***a***: CH_3CN, reflux, 2h; ***b:*** H_2, Pd/C, 50 psi, r.t., 4h.

In order to evaluate if the pure enantiomers possess different biological activity and if this can be related to the absolute configuration, we synthesized some of the selected compounds in the enantiomerically pure form. The pure enantiomers of esters **1** and **2** and carbamates **5**, **6** and **8** were obtained as described for racemates from enantiomerically pure *R* or *S* 1-(4-fluorophenyl)-2-(1H-imidazol-1-yl)ethanol and *R* or *S* 1-(4-chlorophenyl)-2-(1H-imidazol-1-yl)ethanol, as previously reported [12].

2.2 Antiparasitic activity

All compounds were *in vitro* tested *vs* amastigote stage of *T. cruzi*, Tulahuen CL2, β-galactosidase strain (nifurtimox-sensitive). In addition the screening was extended to include the activity of compounds **1-8** towards the other human protozoan parasites *Leishmania infantum* (MHOM/MA-BE/67 amastigotes), *T. brucei* (Squib-427 strain, suramin-sensitive) and *Plasmodium falciparum* (Chloroquine-resistant K1-strain). The *in vitro* screening was carried out according to the previously described procedures [18]. The results are reported in **Table 1**. All the racemic azole derivatives show an anti-*T. cruzi* activity with IC_{50}-values ranging from 0.04 to 5.84 μM. In particular, **1**, **2**, **5-8** were more active than benznidazole used as reference drug. The most active compound **7** showed IC_{50} values of 40 nM and it proved to be approximately fifty times more active than benznidazole and eight times less active than azole reference compound, posaconazole (Table 1).

Table 1. *In vitro* antiparasitic activity and cytotoxicity of compounds **1-8.**

Cmp	***Tc***[a]	***Li***[c]	***Tb***[d]	***Pf***[e]	***MRC-5***[f]	***SI***[g]	***LogP***[h]
1	0.48	12.7	32.4	1.9	7.2	15.0	5.963
(R)-1	0.20	>64.0	32.4	2.0	7.8	39.0	
(S)-1	0.56	32.0	30.1	2.1	8.2	14.6	
2	0.71	32.2	32.2	0.6	7.8	10.9	5.662
(R)-2	1.80	>64.0	>64.0	2.3	>64	>35.6	
(S)-2	0.49	34.6	33.7	2.0	8.0	16.3	
3	2.72	8.0	29.1	7.7	8.8	3.2	7.236
4	5.84	>64.0	>64.0	10.7	>64.0	>10.9	3.775
5	0.87	8.0	8.0	2.4	8.2	9.4	4.405
(R)-5	1.00	12.7	32.2	2.2	8.7	8.7	
(S)-5	1.32	12.7	>64	1.5	8.5	6.4	
6	1.68	27.2	27.2	2.6	15.5	9.2	4.138
(R)-6	1.23	20.3	32.2	1.2	8.7	7.0	
(S)-6	5.44	>64	>64	1.3	8.2	1.5	
7	0.04	38.0	>64.0	17.2	>64	>1600	4.096
8	0.79	28.9	32.9	4.0	26.4	33.4	5.011
(R)-8	1.72	>64	>64	4.0	26.5	15.4	
(S)-8	0.13	>64	>64	5.2	37.5	288.5	
BNZ	1.95	-	-	-	-	-	
MIL	-	10.4	-	-	-	-	
SUR	-	-	0.02	-	-	-	
CHL	-	-	-	0.14	-	-	
TAM	-	-	-	-	10.9	-	
POS	0.005 [b]						

Data represent IC_{50}-values given in µM. *a*: *T.cruzi* Tulahuen CL2 amastigote stage; *b*: Ref 13; *c*: *L. infantum* MHOM/MA/67/ITMAP263; *d*: *T. brucei rhodesiense* Squib-427 strain, suramin-sensitive, trypomastigote stage; *e: P. falciparum* K1, Chloroquine-resistant, erythrocytic stages; *f*: Human fetal lung fibroblast (MRC-5) cell line toxicity; *g*: selectivity index calculated as $IC_{50MRC-5}/IC_{50Tc}$*; h:* LogP were calculated by QikProp ver. 4.2 [18]; *BNZ = benznidazole, MIL = miltefosine; Sur = suramin; CHL = chloroquine; TAM = tamoxifen; POS = posaconazole.*

The antiparasitic activity and cytotoxicity data show that the imidazole derivatives **1-8** are highly selective towards *T. cruzi*. In particular, compound **7** possess the highest activity (*T. cruzi* IC_{50} 0.04 µM) and the lowest cytotoxicity (MRC-5 IC_{50} > 64 µM and a SI >1600), making it an excellent candidate for a new series of anti-Chagas imidazole derivatives.

Compounds **1**, **3** and **5** presented an antileishamial activity similar to miltefosine but they showed a cytotoxicity on MRC-5 cell line of the same magnitude, thus indicating the lack of selectivity towards *L. infantum*.

Furthermore, compound **2** showed antiplasmodial activity (IC_{50} 0.6 µM), approximately twice than the reference drug chloroquine, and good selectivity against *P. falciparum*, with an low cytotoxicity vs MRC-5 cell (MRC-5 IC_{50} 7.8 µM).

None of studied azole compounds showed a higher or comparable activity than the reference drug suramine towards *T. brucei*, which generally demonstrates lower sensitivity vs this class of compounds.

The high selectivity of studied compounds toward *T. cruzi* over *T. brucei* and *L. infantum* could be probably due also to the difference in the CYP51 active site volume and surface area smaller in *T. brucei* and *L. infantum* than in *T. cruzi* that could favour the access of drugs in the active site. [12]

The analysis of the anti-Chagas activity data of the pure enantiomers highlights two significant aspects: i) in all cases, we found a small difference in activity in a pair of enantiomers reaching maximum one order of magnitude; ii) the most active enantiomers do not have the same absolute configuration, for compound **1**, **5** and **6** we found that the most active was the *R*-enantiomer, on the contrary, for compounds **2** and **8,** *S* resulted the most active enantiomer. These results are in good agreement with our previously reported data for similar compounds [13], which showed that both enantiomers of are able to bind and inhibit the $CYP51_{Tc}$.

2.3 Molecular docking

To rationalize the effect of different side chains on the $CYP51_{Tc}$ as the target protein, due to the high structural similarity to previously reported CYP51 inhibitors [13], a docking study was performed. Recently, $CYP51_{Tc}$ was solved with the compounds LFT (**IIa**), LFS (**IIb**) and LFD (**III**), (PDB ID: 4CK9, 2.74 Å resolution; 4CKA, 2.70 Å resolution; 4CK8, 2.62 Å resolution) [13]. The coordinates of $CYP51_{Tc}$ co-crystallized with **III** (PDB ID: 4CK8) were downloaded from the Protein Data Bank (PDB) because of the highest resolution, and used for the subsequent docking studies. The enzyme structure was pretreated by means of the *Protein Preparation Wizard* of Maestro9.9 suite [20], deleting crystallization water molecules, adding hydrogen atoms, filling in missing side chains, and assigning the correct ionization state of the co-crystallized ligands at physiological pH (7 ± 2.0) using *Epik*2.9 [21], and the correct amino acids protonation state at the same pH using *Prime* [22]. The azole derivatives were designed by means of Maestro9.9 and

pretreated with *LigPrep*3.1 [23]. Their ionization state was checked at physiological pH (7 ± 2.0) using *Epik*2.9. Since all compounds have a chiral center, the molecular modeling study was performed considering both –*R* and –*S* enantiomers. Docking studies were performed in the active site of the pretreated $CYP51_{Tc}$ by means of *Glide*6.4 [24], using the Standard Precision (SP) scoring function. Docking protocol was validated reproducing the co-crystal binding pose of the compound III (Supportive information). The protein-ligand interaction energy (PLIE) was estimated for the selected docking poses by means of SZYBKI 1.8.0.1 [25] using the Poisson-Boltzmann solvation model.

The only difference between compounds **1** (IC_{50} = 0.48 µM) and **2** (IC_{50} = 0.71 µM) and the already tested 2-(1*H*-imidazol-1-yl)-1-phenylethyl biphenyl-4-carboxylate (**I,** IC_{50} = 0.014 µM *vs T. cruzi* amastigote stage cells) [12] is the substitution of the hydrogen atom by a chlorine in compound **1** and by a fluorine in compound **2**. Both the halogens are oriented towards a little hydrophobic cavity formed by A287, F210, Y116 and L127. The lone pair oxygen of Y116 faces the halogens atoms in both compounds' poses. Hence, the decrease in the activity of compounds 1 and 2 with respect to compound **I** can be ascribed to a little electron repulsion effect between F and Cl and the Y116 lone pair oxygen.

The further decrease of *T. cruzi* inhibition exerted by compound **3** (IC_{50} = 2.72 µM) could be ascribed to a worse coordination at the heme iron, compared to that of the other more active compounds (Figure 1), since the coordination angle between the lone pair N of the azole ring and the iron should be perpendicular [13]. In addition the protein-ligand interaction energy (PLIE) is not so favored: the R-enantiomer shows a PLIE = -5.17 kcal/mol and the S enantiomer a PLIE = 0.31 kcal/mol. Since the activity is referring to the racemic mixture, we can consider an average of -2.43 kcal/mol.

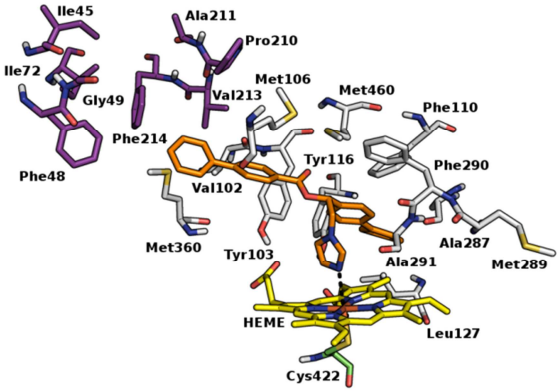

Figure 1: compound **(*R*)-3** docking binding pose (orange stick). The hydrophobic cavity surrounding the heme prosthetic group is shown in gray stick and the HC2 in purple stick. Cys422 coordinating the heme iron is represented in light green stick and the heme prosthetic group in yellow stick. Coordination at the heme iron is represented as black dotted lines. Atoms are colored according to their atom types and non-polar hydrogen atoms are omitted.

Compound **4** (IC_{50}=5.84 µM) shows both a Cl inserted in the little hydrophobic cavity as described for compounds 1 and 2, and also a furanyl moiety with lone pair oxygen oriented towards the lone pair S of M360 in the **(*R*)-** enantiomer and towards the backbone oxygen of Val102 in the **(*S*)-** enantiomer, that can contribute to the decrease of its activity due to a repulsive effect (Figure 2). Indeed, the PLIE for its S enantiomer is in a positive range (+3.21 kcal/mol) and for the R enantiomer is reasonable (-9.91 kcal/mol), but the IC_{50} is referring to the racemic mixture, hence we can consider an average of -3.35 kcal/mol. Compounds **5** (IC_{50} = 0.87 µM) and **6** (IC_{50} = 1.68 µM) are characterized by a NO_2 group that decreases their overall hydrophobicity and hence the permeability through parasite's cell membrane, being a reasonable explanation of the decrease of activity, even if the docking study indicates a good coordination at the heme iron and seem to be well stabilized in the active site of the enzyme by hydrophobic interactions into the hydrophobic cavity surrounding the prosthetic group, as also shown by the favored PLIE values (Figure 2, Table 2). In addition, in compound **6**, the para-Cl substituent at the phenyl ring is replaced by a para-F substituent that can further contribute to the decrease of the overall hydrophobicity of the compound.

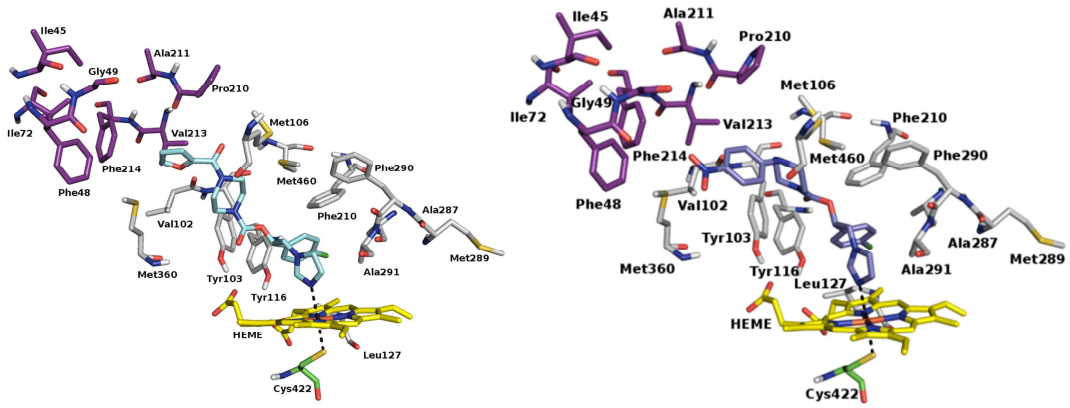

Figure 2: docking binding pose of compound **(*S*)-4** (left, cyan stick) and **(*S*)-5** (right, pale violet stick). Color code is according to Figure 1.

The docking pose of the most active compounds **7** and **8** (Figure 3) shows that their side chain explores a cavity surrounding the prosthetic group, formed by Ile45, Phe48, Gly49, Ile72, Pro210, Ala211, Val213, Phe214 (for convenience thereafter referred to HC 2), showing a similar binding mode to that of the co-crystallized **III**. This evidence together with their higher hydrophobicity and the very low PLIE value could explain their high activity.

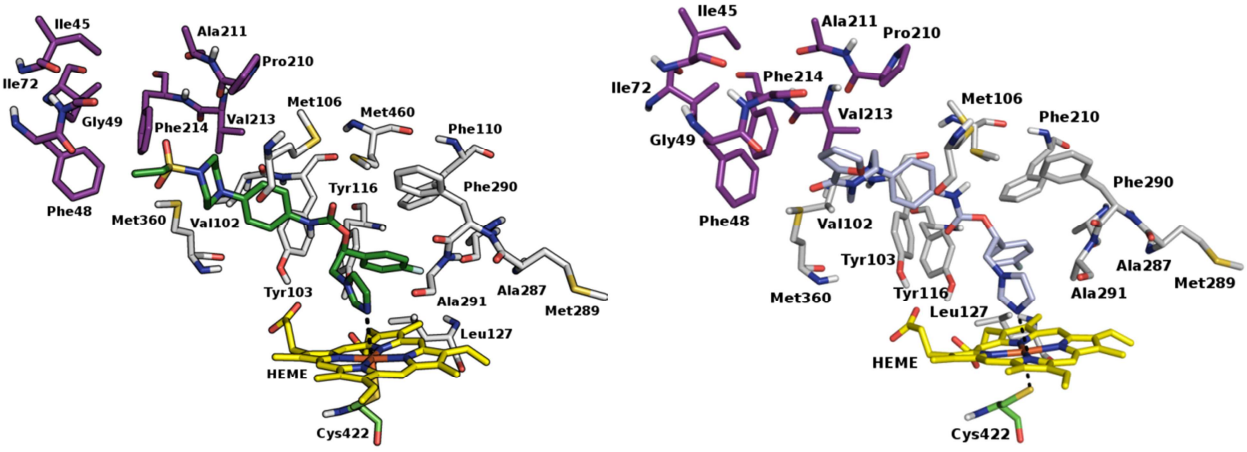

Figure 3: docking binding pose of the most active compounds **(*S*)-7** (left, green stick) and **(*R*)-8** (right, pale cyan stick). Color code is according to Figure 1.

Table 2. Protein-Ligand interaction energy values (PLIE) of the different enantiomers binding poses in CYP41 4CK8 coordinates

Compound	PLIE (kcal/mol)
(*R*)-**1**	-9.34
(*S*)-**1**	-1.87
(*R*)-**2**	-10.30
(*S*)-**2**	-9.53
(*R*)-**3**	-5.17
(*S*)-**3**	0.31
(*R*)-**4**	-9.91
(*S*)-**4**	+3.21
(*R*)-**5**	-6.35
(*S*)-**5**	-3.96
(*R*)-**6**	-4.19
(*S*)-**6**	-4.63
(*R*)-**7**	-14.90
(*S*)-**7**	-22.19
(*R*)-**8**	-11.10
(*S*)-**8**	-25.86

2.4 SAR analysis on anti-*T. cruzi* activity

Due to the high structural similarity of the studied compounds with known $CYP51_{Tc}$ inhibitors and on the basis of our recent publication on X-Ray structures of $CYP51_{Tc}$ co-crystallized with **IIa**, **IIb** and **III,** we judge this enzyme as the target of imidazole derivatives **1-8**. For these reasons, we carried out a docking study and a PLIE estimation to explore their possible binding orientation within the catalytic site of $CYP51_{Tc}$. The results of the modeling study, combined with the hydrophobicity of the side chain, let us to propose a possible explanation of the different biological activity of the studied compounds. From the docking study, it is clear that the coordination at the heme iron is fundamental for the discrimination between active, less active and inactive compounds. Only small hydrophobic groups (chlorine or fluorine) are allowed in the 4 position of the phenyl ring of 1-(phenyl)-2-(1H-imidazol-1-yl)-ethanol derivatives. The replacement of the chlorine with a fluorine atom (**1** *vs* **2** and **5** *vs* **6**) causes only small differences in the antitrypanosomal activity. In general, chloro- derivatives were found to be slightly more active than fluoro- analogues, probably due higher hydrophobicity. The presence of a more bulky phenyl group was detrimental for the biological activity (**3** *vs* **1** and **2**) because of the worst influence on the

heme-iron coordination of the imidazole ring. Otherwise, the presence of a second aromatic ring in the lateral side chain appears to be fundamental as shown by comparing compound **4**, the worse of the series, with compounds **5** and **6**.

The increase in length of the side chain in compounds **7** and **8** compared to **5** and **6** leads to an increase of anti-*T. cruzi* activity. Moreover, the side chains of **7** and **8** are more rigid in the initial part due to the presence of the aromatic ring, and this can orient the chain deeper into the hydrophobic cavity above the heme group.

2.5 Stability studies

Because the synthesized compounds contain ester or carbamate functions, potentially susceptible to hydrolysis, we evaluated the chemical stability of the most active compounds **7** and **8** in acid medium. The possible hydrolysis reaction of **7** and **8** was followed by 1H NMR during 24 hrs at 27 °C in the test tube, dissolving 10^{-4} mol of each compound in 0.6 mL of DCl/D_2O (pH 2). The appearance of the methine and methylene proton signals exclusively related to the alcohol produced by hydrolysis were chosen as a prove of the reaction. For both the compounds **7** and **8**, no free alcohol signals were observed in the experimental conditions thus demonstrating their stability to hydrolysis under the described conditions.

Compounds **7** and **8** were also evaluated for their metabolic stability by treatment with liver microsomal protein. Each compound (50 μM in pH 7.4 phosphate buffer + DMSO 2%) was incubated at 37°C for 60 min with human liver microsomal protein in the presence of a NADPH-generating system. The reaction was stopped and the parent drug and metabolites were determined by LC-UV-MS (see supportive information). Compounds **7** and **8** show high metabolic stability, e.g. 99% of parent drug was not metabolized.

3. CONCLUSIONS

In conclusion, eight imidazole derivatives were evaluated *in vitro* against different parasitic protozoa as racemates and pure enantiomers. The selected compounds showed selective and high activity towards *T. cruzi* amastigotes, with the most active of them, **7**, having an IC_{50} of 40 nM and a low cytotoxicity (MRC-5 IC_{50} > 64 μM). Interesting activity data were also observed against *L. infantum* for the compounds **1**, **3** and **5** and against *P. falciparum* for the compound **2** and may be subject to further investigations.

Furthermore, compound **7** showed a good chemical and metabolic stability, that combined with the simplicity and low cost of its chemical synthesis, make it a good lead for further structural optimization for the anti-Chagas activity.

Acknowledgements

This work was financially supported by Miur, Italy.

References

[1] Investing to overcome the global impact of neglected tropical diseases. Third WHO report on neglected tropical diseases http://www.who.int/neglected_diseases/9789241564861/en/ (last access, 09/25/2015).

[2] F. F. Norman, R. Lopez-Velez, Chagas disease and breast-feeding, Emerg. Infect. Dis. 19(10) (2013) 1561-1566; DOI: 10.3201/eid1910.130203.

[3] K. M. Bonney, Chagas disease in the 21st Century: A public health success or an emerging threat? Parasite. Published on line March 10, 2014; DOI: 10.1051/parasite/2014012.

[4] A. Jr. Rassi, A. Rassi, J. A. Marin-Neto, Chagas Disease. Lancet 375(9723) (2010) 1388-1402; DOI: 10.1016/S0140-6736(10)60061-X.

[5] J. A. Urbina, Recent Clinical Trials for the Etiological Treatment of Chronic Chagas Disease: Advances, Challenges and Perspectives. J. Eukaryot. Microbiol. 62 (2015) 149-156. DOI: 10.1111/jeu.12184.

[6] J. M. Bustamante, R.L. Tarleton, Potential new clinical therapies for Chagas disease. Expert Rev. Clin. Pharmacol. 73(3) (2014) 317-325. DOI: 10.1586/17512433.2014.909282.

[7] M. T. Bahia, L. de Figueiredo Diniz, V.C. Furtado Mosqueira, Therapeutical approaches under investigation for treatment of Chagas disease. Expert Opin. Inv. Drug 23(9) (2014) 1225-1237; DOI: 10.1517/13543784.2014.922952.

[8] F.S. Buckner, J. A. Urbina, Recent developments in sterol 14-demethylase inhibitors for Chagas disease. Int. J. Parasitol-Drug 2 (2012) 236-242; DOI: 10.1016/j.ijpddr.2011.12.002.

[9] C.W. Roberts, R. McLeod, D. W. Rice, M. Ginger, M. L. Chance, L. J. Goad, Fatty acid and sterol metabolism: Potential antimicrobial targets in apicomplexan and trypanosomatid parasitic protozoa. Mol. Biochem. Parasit. 126 (2003) 129-142; DOI: 10.1016/S0166-6851(02)00280-3.

[10] E. Chatelain, Chagas Disease Drug Discovery: Toward a New Era. J. Biomol. Screen. 20(1) (2015) 22-35; DOI: 10.1177/1087057114550585.

[11] J. Y. Choi, L. M. Podust, W. R. Roush, Drug Strategies Targeting CYP51 in Neglected Tropical Diseases. Chem. Rev. 114 (2014), 11242-11271; DOI: 10.1021/cr5003134.

[12] L. Friggeri, L. Scipione, R. Costi, M. Kaiser, F. Moraca, C. Zamperini, B. Botta, R. Di Santo, D. De Vita, R. Brun, S. Tortorella, New promising compounds with in vitro nanomolar activity against *Trypanosoma cruzi*. ACS Med. Chem. Lett. 6 (2013) 538-541; DOI: 10.1021/ml400039r.

[13] L. Friggeri. T. Y. Hargrove, G. Rachakonda, A. D. Williams, Z. Wawrzak, R. Di Santo, D. De Vita, M. R. Waterman, S. Tortorella, F. Villalta, G. I. Lepesheva, Structural basis for rational design of inhibitors targeting *Trypanosoma cruzi* Sterol 14α-demethylase: Two regions of the enzyme molecule potentiate its inhibition. J Med. Chem. 57(15) (2014) 6704-6717; DOI: 10.1021/jm500739f.

[14] F. Moraca, D. De Vita, F. Pandolfi, R. Di Santo, R. Costi, R. Cirilli, F. D. D'Auria, S. Panella, A. T. Palamara, G. Simonetti, M. Botta, L. Scipione, Synthesis, biological evaluation and structure-activity correlation study of a series of imidazol-based compounds as *Candida albicans* inhibitors Eur. J. Med. Chem. 18(83) (2014) 665-673; DOI: 10.1016/j.ejmech.2014.07.001.

[15] D. De Vita, L. Scipione, S. Tortorella, P. Mellini, B. Di Rienzo, G. Simonetti, F. D. D'Auria, S. Panella, R. Cirilli, R. Di Santo, A. T. Palamara, Synthesis and antifungal activity of a new series of 2-(1H-imidazol-1-yl)-1-phenylethanol derivatives. Eur. J. Med. Chem. 49 (2012) 334-342; DOI: 10.1016/j.ejmech.2012.01.034.

[16] S. Patterson**,** M. S. Alphey, D. C. Jones, E. J. Shanks, I. P. Street, J. A. Frearson, P. G. Wyatt, I. H. Gilbert, A. H. Fairlamb, Dihydroquinazolines as a novel class of *Trypanosoma brucei* trypanothione reductase inhibitors: Discovery, synthesis, and characterization of their binding mode by protein crystallography. J. Med. Chem. 54 (2011) 6514-6530; DOI: 10.1021/jm200312v.

[17] J. C. Engel, K. K. H. Ang, S. Chen, M. R. Arkin, J. H. McKerrow, P. S. Doyle, Image-based high-throughput drug screening targeting the intracellular stage of *Trypanosoma cruzi*, the agent of Chagas' disease. Antimicrob. Agents Chemother. 54(8) 2010 3326-3334; DOI: 10.1128/AAC.01777-09.

[18] P. Cos, A. J. Vlietinck, D. V. Berghe, L. Maes, Anti-infective potential of natural products: how to develop a stronger in vitro 'proof-of-concept'. J. Ethnopharmacol. 106(3) (2006) 290-302; DOI: 10.1016/j.jep.2006.04.003.

[19] QikProp, version 4.2, Schrödinger, LLC, New York, NY, 2014

[20] Maestro, version 9.9, Schrödinger, LLC, New York, NY, 2014.

[21] Epik, version 2.9, Schrödonger, LLC, New York, NY, 2014.

[22] Prime, version 3.7, Schrödonger, LLC, New York, NY, 2014.

[23] LigPrep, version 3.1, Schrödinger, LLC, New York, NY, 2014

[24] Glide, version 6.4, Schrödinger, LLC, New York, NY, 2014

[25] S. Wlodek, A. G. Skillman, A. Nicholls, Ligand entropy in gas-phase, upon solvation and protein complexation. Fast estimation with Quasi-Newton Hessian. J. Chem. Theory Comput. 6(7) (2010) 2140-2152; DOI: 10.1021/ct100095p.